

DIRECT OBSERVATION OF THE α - ϵ TRANSITION IN SHOCKED SINGLE CRYSTAL IRON

D. H. Kalantar¹, G. W. Collins¹, J. D. Colvin¹, H. M. Davies²,
 J. H. Eggert¹, J. Hawreliak¹, H. E. Lorenzana¹, M. A. Meyers³, K. Rosolankova⁴,
 M. S. Schneider³, J. Sheppard⁴, J. S. Stölken¹, J. S. Wark⁴

¹*Lawrence Livermore National Laboratory, Livermore, CA 94550*

²*AWE Aldermaston, Reading, RG7 4PR, UK*

³*University of California at San Diego, La Jolla, CA 92093*

⁴*Department of Physics, Clarendon Laboratory, University of Oxford, Oxford, OX1 3PU, UK*

Abstract. *In-situ* x-ray diffraction was used to study the response of single crystal iron under shock conditions. Measurements of the response of [001] iron showed a uniaxial compression of the initially bcc lattice along the shock direction by up to 6% at 13 GPa. Above this pressure, the lattice responded with a further collapse of the lattice by 15-18% and a transformation to the hcp structure. The *in-situ* measurements are discussed and results summarized.

Keywords: *in-situ* diffraction, laser shocks, phase transformation, iron.

PACS: 64.70.-p, 07.35.+k, 61.10.-i, 63.90.+t.

INTRODUCTION

The crystallographic structure of a solid is one of its fundamental properties. This structure may undergo a transformation due to high-pressure loading. Bridgman showed that many crystals undergo structural transformations under static high pressure. [1] Pressure-induced transformations in materials such as iron were also reported under shock loading. A structural transformation in iron was predicted at about 13 GPa based on wave profile measurements in shock experiments. [2, 3] This transformation was later identified as the α - ϵ transition, which was subsequently observed to occur at this pressure in static experiments. [4]

We present experimental results from *in-situ* diffraction measurements of shocked single crystal iron. These results provide a *direct* confirmation of this phase transformation in shocked iron. This is

also consistent with previous experiments to determine the transition time of the transformation, where iron samples were shock loaded and recovered. Residual deformation analysis showed evidence of the transformation to the hcp phase on the nanosecond time-scale. [5-8]

IN-SITU DIFFRACTION

In-situ diffraction is applied in laser-based experiments using a monochromatic x-ray source located close to the surface of a single crystal sample. The x-rays are created by direct laser irradiation of a metal foil. They are incident on the single crystal sample at a wide range of angles, satisfying the Bragg diffraction condition

$$n\lambda = 2d \sin(\theta) \quad (1)$$

for different lattice planes at different locations in the crystal. Here, λ is the x-ray wavelength, d is the lattice spacing, and θ is the Bragg diffraction angle.

The geometry for the laser experiments is shown in Fig. 1. The single crystal sample is located approximately 1.3 mm from the thin iron backlighter foil. High intensity irradiation of a parylene ablation layer with a focal spot size of 2.5 mm provides the pressure source for shock loading. X-rays diffracted from multiple lattice planes of the crystal are recorded on a wide-angle film detector that subtends up to a full π -steradian solid angle.

The single crystal [001] iron samples used in these experiments were 200 μm thick, obtained from Accumet Materials and overcoated with a 16-20 μm parylene-N ablator layer and 0.1 μm aluminum shine-through layer. They were shock loaded by direct laser irradiation at intensities from 2×10^{10} to 1×10^{12} W/cm^2 using 2-6 nanosecond constant intensity laser pulses with laser wavelengths of 351 nm, and 532 nm using the OMEGA [9] and Janus lasers. Additional experiments were conducted using 10 μm thick single crystal samples of iron fabricated by vapor deposition and driven with a laser wavelength of 1064 nm using the Vulcan laser [10].

Iron K-shell x-rays with a wavelength of 1.85 \AA were used for the diffraction measurements. The x-rays were incident on the crystal at a range of angles, diffracting from many different lattice planes and recorded as line features on film. [11]

THE α - ϵ TRANSITION IN IRON

The transition from bcc to hcp involves a volume collapse, and systematic shift of atoms in the lattice. For a single crystal that is subjected to

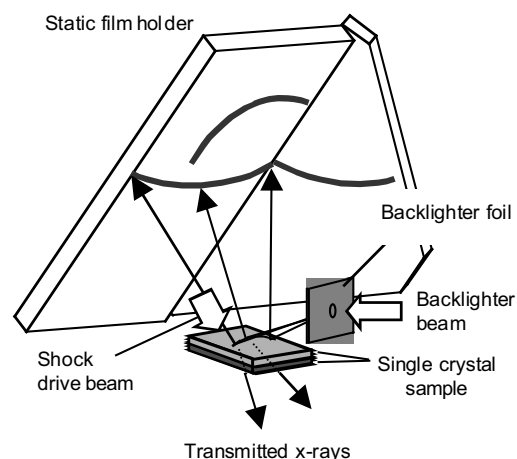


Fig. 1: Experimental geometry for laser-based in-situ diffraction experiments of shocked samples.

strain along the [001] direction, there have been several mechanisms proposed for this transition in iron based on an applied stress along the [001] direction. In this discussion, we focus on only the first mechanism that is summarized by Wang and Ingalls. [12] This transformation mechanism involves a simple uniaxial compression and a shuffling of alternate (110) planes of atoms. A compression of the initially bcc lattice by 18.4% along the [001] direction places atoms from the (110) planes into perfect hexagons. Then an additional shuffling of alternate (110) planes by $a/3\sqrt{2}$, where a is the spacing of the initial bcc

lattice, establishes the atomic ordering of a pseudo-hcp lattice whose c-axis corresponds to the [-110] direction in the initial structure (Fig. 2). Note that this is not a true hcp lattice since the final lattice configuration has a different a/c ratio from the true hcp structure.

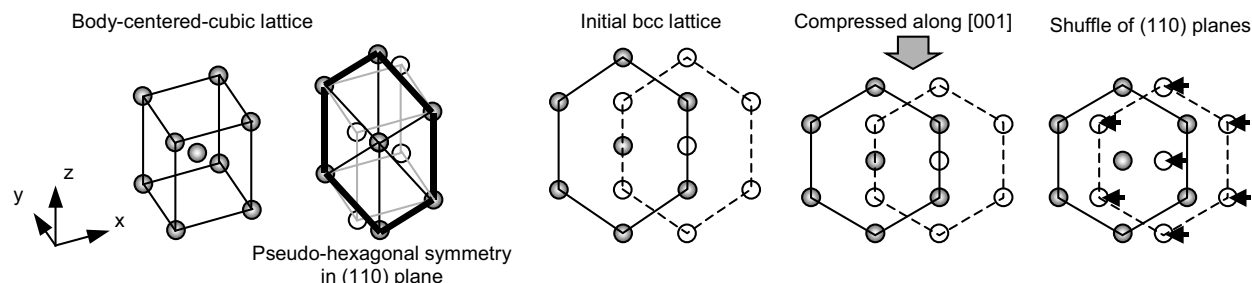


Fig. 2: Illustration of the transformation from the initially bcc lattice to hcp by compression along the [001] direction and shuffling of alternate (110) planes.

EXPERIMENTAL RESULTS

The response of [001] single crystal iron samples was measured at laser drive conditions that span the α - ϵ transition pressure. One sample diffraction image is shown in Fig. 3. This image shows x-ray diffraction lines from both the uncompressed and compressed lattice recorded as the shock propagated through the crystal in a reflection Bragg geometry. This image was recorded with a pressure of approximately 26 GPa,

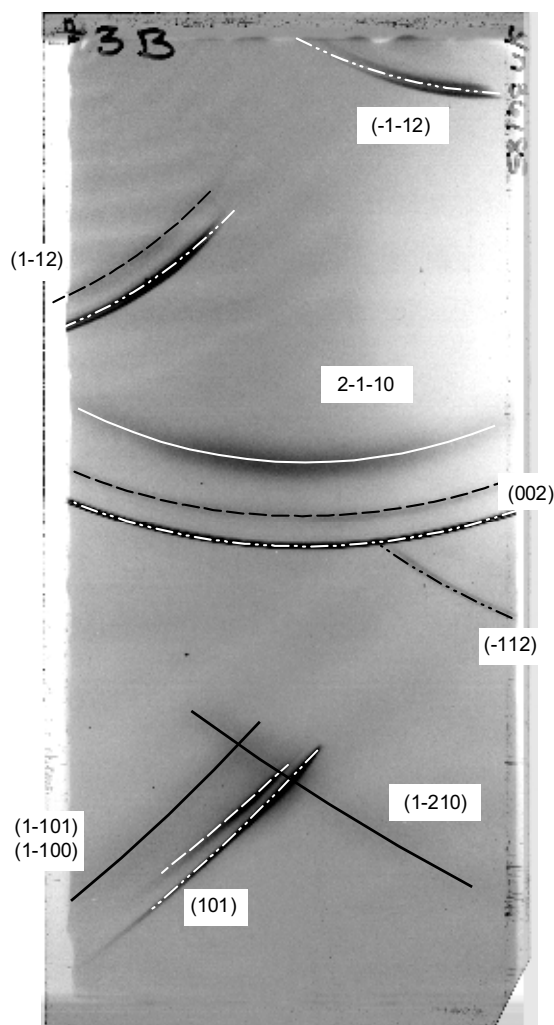


Fig. 3: Example diffraction data from shocked single crystal [001] iron showing diffraction curves from the static bcc lattice (dash-dot), uniaxially compressed bcc lattice (dash), and hcp lattice (solid). The different compressions are visible in the same image due to time-integration of the measurement during shock loading.

achieved with a laser intensity of $3.1 \times 10^{11} \text{ W/cm}^2$ at 351 nm irradiation wavelength. At this pressure, multiple compression features are evident due to both the static and compressed lattice. In these experiments, the x-ray diffraction probe has a duration of 2-4 ns, spanning the time that the sample is shock loaded by direct laser irradiation.

The diffraction pattern from the static (unshocked) bcc lattice is identified with dash-dot overlays. The narrow shifted lines are identified with a dashed overlay. These lines correspond to diffraction from a uniaxially compressed bcc lattice. The displacement of the (002) diffraction line in the image shown in Fig. 3 is consistent with a compression of 6.0% along the [001] shock direction. The corresponding displacement of the diffraction lines from the $(\pm 1-12)$ and (± 101) lattice planes indicate a compression 5.5 and 5.9% along the [001] direction.

Additional diffuse shifted diffraction lines appear associated with the (002) and (± 101) lattice planes. The shift of these lines on the film indicates compression of the lattice along the [001] direction by 15-18%. An additional diffuse diffraction line appears that does not have a corresponding static line in Fig. 3. This new line, and other lines that appear in transmission diffraction images [13] require the symmetry of an hcp structure to exist. The new feature shown in Figure 3b is identified with diffraction from the (1-210) lattice planes of hcp iron.

The collapse of the lattice along the [001] direction and the appearance of the new lines in both reflection and transmission Bragg diffraction are consistent with the transformation to the hcp phase.

The compression of the lattice along the shock direction is plotted as a function of pressure in Fig. 4. Here, the lattice spacing was determined from the shift of the (002) planes, since they are parallel to the shock direction. This uniaxial deformation up to 6% has an uncertainty of approximately 0.003. The 15-18% compressions have an uncertainty of approximately 0.01-0.02.

Scaling of the pressure with wavelength and intensity to relate the experiments conducted at the different laser facilities was based on simulations using the 2D radiation-hydrodynamics code LASNEX [14]. The calibration of the pressure

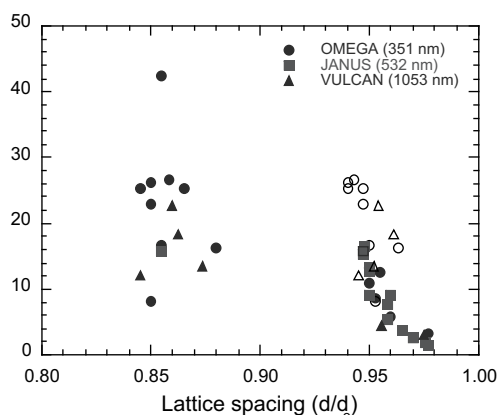


Fig. 4: Iron lattice compression inferred from shift of the (002) diffraction line vs. laser intensity (shock pressure).

scale was established based on the third order elasticity constants for iron. [15-16]

The data shown in Fig. 4 shows a discontinuity consistent with a volume collapse and phase transformation at approximately 13 GPa. Above this pressure, two compressions were observed. The lower compression is consistent with uniaxial distortion of the initially bcc lattice, and does not change with pressure (laser intensity). The higher compression is consistent with the further collapse of the lattice and transformation to hcp. Both compressions are shown on the plot to indicate their simultaneous presence in the measurements.

SUMMARY

In conclusion, we have used the technique of nanosecond *in-situ* x-ray diffraction to confirm that iron indeed transforms to an hcp structure under shock loading. Single crystal iron that is shock loaded along the [001] direction undergoes a uniaxial compression, followed by a transformation to the hcp phase. In both the compressed bcc phase, and the new hcp phase, there is low strain transverse to the shock propagation direction. The capability to directly observe atomic motion under shock compression with the technique of *in-situ* diffraction offers the potential to greatly extend our knowledge of the mechanisms underlying many more shock-induced phase transformations.

ACKNOWLEDGEMENTS

This work was conducted under the auspices of the US DOE by the UC LLNL under Contract No. W-7405-Eng-48. Experiments were conducted at the University of Rochester Laboratory for Laser Energetics under the NLUF grants program. Additional support was provided by DOE grants DEFG0398DP00212 and DEFG0300SF2202, by the UK EPSRC Grant GR/R25699/01, and by the LDRD program project 04-ERD-071 at LLNL.

REFERENCES

- 1 Bridgman, P. W., Collected Experimental Papers (Harvard University Press, Cambridge, MA, 1964).
- 2 Walsh, J. M., Bull. Am. Phys. Soc. **29**, 28 (1954).
- 3 Bancroft, D., Peterson, E. L., and Minshall, S., J. Appl. Phys. **27**, 291 (1956).
- 4 Jamieson, J. C., Lawson, A.W., J. Appl. Phys. **33**, 776 (1962).
- 5 Smith, C. S., Trans. AIME **214**, 574 (1958).
- 6 Forbes, J. W., PhD Thesis, Washington State University, 1976 & Naval Surface Weapons Centre Report NSWC/WOL TR 77-137, 1977.
- 7 Duvall, G. E., Graham, R. A., Rev. Mod. Phys. **49**, 523 (1977).
- 8 Sano, T., Mori, H., Ohmura, E., and Miyamoto, I., Appl. Phys. Lett. **83**, 3498 (2003).
- 9 Boehly, T. R., Craxton, R. S., Hinterman, T. H., *et al*, Rev. Sci. Instrum. **66**, 508-510 (1995).
- 10 Danson, C. N., Barzanti, L., Chang, Z., *et al*, Opt. Commun. **103**, 392 (1993).
- 11 Kalantar, D. H., Bringa, E., Caturla, M., *et al*, Rev. Sci. Instrum. **74**, 1929 (2003).
- 12 Wang, F. M., Ingalls, R., Phys. Rev. B, **57**, 5647 (1998).
- 13 Kalantar, D. H., Belak, J. F., Collins, G. W., *et al*, Phys. Rev. Lett. **95**, 075502 (2005).
- 14 Zimmerman, G. B., Kruer, W. K., Comments Plasma Phys. Control. Fusion **2**, 51 (1975).
- 15 Landolt-Bornstein, "Numerical Data and Functional Relationships in Science and Technology – Group III", Crystal and Solid State Physics, Vol. 11, 1979.
- 16 Ritchie, A. D., "Anharmonicity in Alpha-Iron: The Third-Order elastic Coefficients", Ph. D. Thesis, University of California at Davis, 1969, and LLNL Technical Document, UCRL-50548.